

¹⁷P. W. M. Glaudemans, G. Wiechers, and P. J. Brusard, *Nucl. Phys.* **56**, 529, 548 (1964).

¹⁸M. C. Bouten, J. P. Elliott, and J. A. Pullen, *Nucl. Phys.* **A97**, 113 (1967).

¹⁹B. P. Singh, B. Castel, I. P. Johnstone, and K. W. C.

Stewart, *Phys. Rev. C* **5**, 1613 (1972).

²⁰H. Rebel *et al.*, *Phys. Rev. Letters* **26**, 1190 (1971).

²¹B. Lawergren, I. J. Taylor, and M. Nessin, *Phys. Rev. C* **3**, 994 (1970).

Elastic Scattering of Alpha Particles from ²⁷Al in the Energy Range 21–28 MeV*

K. W. Kemper, A. W. Obst, and R. L. White

Department of Physics, The Florida State University, Tallahassee, Florida 32306

(Received 5 July 1972)

60-point angular distributions have been measured in 200-keV steps for ²⁷Al(α , α_0)²⁷Al in the energy range 21–28 MeV. At an incident energy of 23.9 MeV an anomalous structure of full width at half maximum \sim 300 keV is seen for angles greater than 90°, but above 25 MeV no correlated structure is seen. The data above 25 MeV have been analyzed in terms of the optical model, and discrete potential ambiguities, as well as a radius ambiguity, have been found. These potential parameter sets were able to give qualitative fits to the data throughout the angular range 25–150° (c.m.) at the energies 24.9, 25.9, and 27.5 MeV, and at the lower energies 22.3 and 23.3 MeV the general trend of the data was reproduced.

I. INTRODUCTION

As part of a study of α -particle induced-reactions on ²⁷Al, the elastic scattering of α particles by ²⁷Al has been measured in the laboratory energy range 21–28 MeV. The objective of this work was to obtain optical-model parameters for use in future distorted-wave Born-approximation calculations of the reactions under study.

Initially, it was thought this study would not be necessary, since earlier studies¹ indicated that α scattering by ²⁷Al is direct above 17 MeV and a complete angular distribution has been measured² for $E_\alpha = 18.82$ MeV as well as a partial angular distribution ($\theta_{\text{lab}} < 90^\circ$) for $E_\alpha = 28$ MeV.³ Attempts to describe the 19-MeV data with the optical model by Srivastava and Johnson⁴ were unsuccessful for $\theta_{\text{c.m.}} > 80^\circ$, where the data were higher than the calculations. An analysis of the 28-MeV data by Satchler⁵ shows a similar feature. This result is not surprising, since for several other⁶ *2s-1d* shell nuclei nondirect contributions to the cross section have been found to be important for angles greater than 90° in this energy range. To determine whether nondirect contributions are present at tandem energies for α scattering from ²⁷Al, excitation functions and angular distributions are reported for α particles of energy 21–28 MeV. The results of an optical-model analysis of the data are also presented.

II. EXPERIMENTAL PROCEDURE

The Florida State University FN tandem Van

de Graaff was used to accelerate ⁴He⁻ ions and typical beam currents were 150–300 nA. The two targets used in this work were rolled foils whose thicknesses were 200 and 50 keV for 25-MeV α particles. Since the ¹⁹⁷Au(α , α_0)¹⁹⁷Au excitation function does not exhibit any radical fluctuations in the energy range covered here⁷ a flash of gold evaporated on the targets was used to provide a continuous system check. The detector solid angles were determined by scattering 6-MeV α particles from a gold target whose thickness was determined by the energy loss of α particles from an ²⁴¹Am source.

Differential cross sections were measured at 16 angles simultaneously with Si-surface-barrier detectors mounted in a ring which was contained in a 45-cm scattering chamber.⁸ The data were accumulated in a TMC 4096-channel analyzer coupled to an EMR-6130 computer for on-line data analysis. By adjustment of the beam current, the dead time of the analyzer was kept to less than 10%.

The systematic error in the data estimated from the reproducibility of the data obtained in different runs is 3% and is due to uncertainties in the beam-current integration and the solid-angle determinations. The statistical uncertainty was always less than 3% and the absolute error assigned to each data point was between 4 and 5%.

III. EXPERIMENTAL RESULTS

The data reported here consist of excitation functions in the bombarding energy range from

21 to 28 MeV taken in steps of 200 keV. The angular range investigated was 20 – 170° (lab) in 2.5° steps. These data were taken with the 200-keV-thick target so that many levels in the compound system would be averaged over. As can be seen in Fig. 1, considerable structure is present below 24.5 MeV, particularly at backward angles. The anomaly at 23.9 MeV has the property of being present at angles greater than 90° with the structure increasing in prominence as the angle increases. Above a bombarding energy of 25 MeV, the structure is less pronounced and no correlated structure is visible at any of the 60 angles for which excitation functions were taken.

To investigate the nature of the anomaly at 24 MeV in greater detail, a 50-keV target was used to measure both elastic and inelastic excitation functions in the energy range from 23.2 to 24.5 MeV. The data are shown in Fig. 2, where α_0 is the elastic scattering, α_{1+2} is the combined scattering from the first and second excited states,

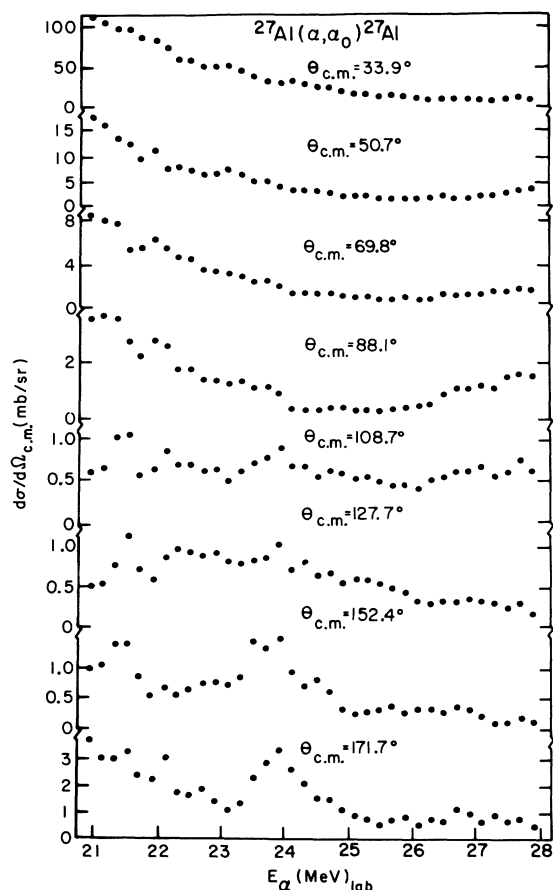


FIG. 1. Selected excitation functions for $^{27}\text{Al}(\alpha, \alpha_0)^{27}\text{Al}$ with a target whose thickness is 200 keV for 25-MeV α particles.

and α_3 is the scattering from the third excited state. The data show no apparent correlation between the elastic and inelastic channels which would seem to rule out trapping states⁹ as the source of the anomaly. Unfortunately, none of the measurements presented here indicate whether the structure is a purely statistical phenomenon, or an intermediate structure effect.

Also shown in Fig. 2 is an excitation function taken in the energy range 26–27 MeV. The decrease in prominent structure in this energy range indicates that corrections for compound-nucleus effects are small and these corrections were not included in the optical-model analysis of the data.

IV. OPTICAL-MODEL ANALYSIS

Optical-model calculations were performed with a modified version of Perey's code JIB¹⁰ for bombarding energies of 24.9, 25.9, and 27.5 MeV. The form of the optical potential employed is shown in Table I. The radius is defined as $R = r_0 A^{1/3}$. The first step in the analysis was to do four-parameter grid calculations ($r_I = r_r$; $a_I = a_r$) for U in the range 10–200 MeV with $\Delta U = 10$ MeV, W in the range 2–20 MeV with $\Delta W = 2$ MeV, r in the range 1.2–1.9 fm with $\Delta r = 0.1$ fm, and a in the range 0.2–0.8 fm with $\Delta a = 0.1$ fm. Grids were also done for an imaginary surface-absorption potential, but no clear choice between the two types of imaginary potentials was apparent and only the volume imaginary potential was used in further calculations. This result is not unexpected, since α -particle scattering at these energies is only sensitive to the tail region of the potential.¹¹

Direct searches were done around each of the minima found in the grid calculations for all three energies simultaneously. At the most backward angles ($>130^\circ$) the calculated cross sections have diffractionlike structure, while the data do not.

TABLE I. Four-parameter optical-model potentials: $V(r) = V_c(r) - (U + iW)(1 + e^{(r-R)/a})^{-1}$, $r_c = 1.70$ fm, $R = r_0 A^{1/3}$, $W = W_1 + W_2 E_\alpha (1 \text{ lab})$.

U (MeV)	W_1 (MeV)	W_2 (MeV)	r_0 (fm)	a (fm)	$\bar{\chi}^2(1)$	$\bar{\chi}^2(2)$
32.3	-1.97	0.45	1.68	0.57	4130	4670
68.3	1.58	0.42	1.58	0.56	3980	5370
108.4	4.81	0.41	1.53	0.53	4160	6720
149.9	5.71	0.47	1.52	0.50	4670	7010
194.5	0.76	0.76	1.53	0.48	5400	6200
64.0	-7.87	0.95	1.31	0.87	4100	5400
114.0	-9.00	1.16	1.25	0.79	4320	5840
165.9	-7.00	1.21	1.23	0.73	4690	6080
217.7	-7.73	1.34	1.24	0.68	5000	6250

This type of behavior has been suggested to be a target-spin effect by Fulmer and Hafele¹² who experimentally compared 50-MeV α -particle scattering from ^{59}Co and ^{60}Ni . Because the form of this spin-dependent potential is not known, no attempt was made to include spin effects in the calculations reported here.

To estimate the compound contribution to the elastic cross section, a Hauser-Feshbach-type calculation was performed using the expressions of Eberhard *et al.*¹³ For angles less than 140° the maximum Hauser-Feshbach contribution was 10% and between 140 and 170° the maximum contribution was 20%. These calculations showed that no serious error was made in the optical analysis by neglecting the compound contribution. A further indication that the compound contribution is small is the ability of the optical potential to yield the proper magnitude of the backward-angle cross section at all three energies, 24.9, 25.9, and 27.5 MeV.

The final four-parameter potentials obtained are

listed in Table I. These potential sets represent the best fit to the data over the whole angular range studied. The energy dependence of the imaginary potential has been parametrized as $W = W_1 + W_2 E_\alpha$ where E_α is the laboratory bombarding energy. Two types of potentials were found, one having a large radius and one having a small radius. This ambiguity in the radius has also been reported by Bobrowska *et al.*¹⁴ who carried out a study of the elastic scattering of α particles by ^{27}Al , ^{28}Si , ^{32}S , Ti, and ^{59}Co at an incident energy of 27.5 MeV. These two potential families do not appear to be related by the Ur^n continuous ambiguity, since the calculated angular distributions have different characteristics. In addition to the ambiguity in the radius, there are also discrete ambiguities which correspond to differing number of nodes in the internal wave function. Typical calculated angular distributions for each type of potential are shown in Figs. 3 and 4.

In Table I, $\chi^2(1)$ is the average total χ^2 value obtained when only the data at 24.9, 25.9, and

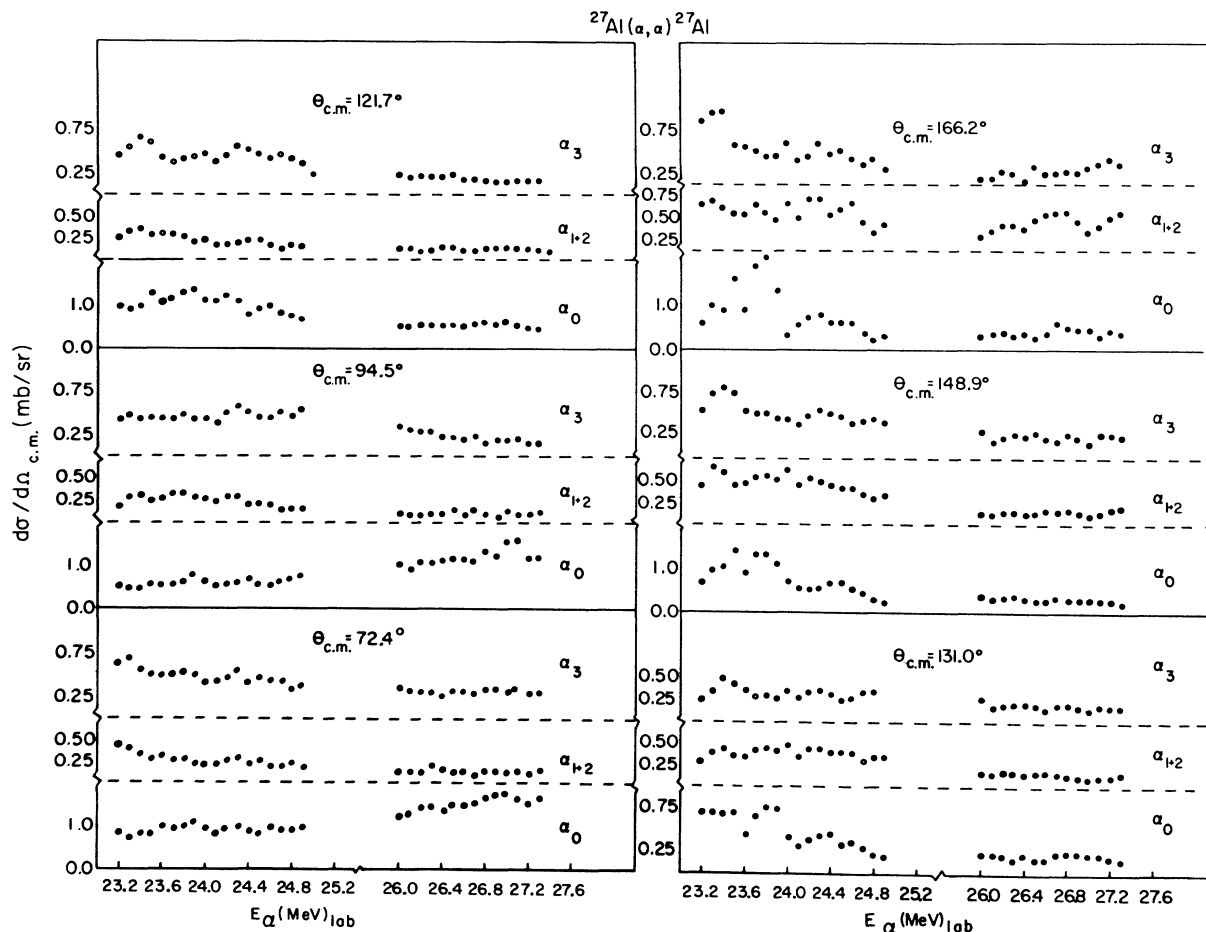


FIG. 2. Selected excitation functions for elastic and inelastic α -particle scattering from ^{27}Al with a target whose thickness is 50 keV for 25-MeV α particles.

27.5 MeV are considered. Calculations have been done for our data with the optical potential parameters found by Bobrowska *et al.*,¹⁴ and the χ^2 for their large radius parameters is typically a factor of 2 larger than those obtained with the parameters of Table I while the small radius parameters yield χ^2 values larger by a factor of 1.5, indicating some preference for the parameters reported here. Calculations were also performed with the parameters of Srivastava and Johnson⁴ and of Satchler.⁵ Both groups of parameters give good fits to the data at all three energies for angles $<75^\circ$, but fall well below the data at angles $>90^\circ$.

Further optical-model calculations were performed with the imaginary and real geometry parameters varied independently. For the large-radius potential parameters the improvement in

χ^2 was about 10% over all, and no real qualitative improvement could be seen. For the small-radius parameters, the average improvement in χ^2 was ~40% and the quality of the fits was markedly improved. Figures 3 and 4 show typical six-parameter fits and Table II lists the six-parameter potentials.

Calculations were carried out for incident α -particle energies of 23.3 and 22.3 MeV to determine if this lower-energy data could be described by the potential parameter sets reported here. These two bombarding energies were chosen because the excitation functions appear to be relatively structureless. The average χ^2 for all five energies is shown as $\chi^2(2)$ in both Tables I and II. For the large-radius parameters a comparison of the χ^2 values in Table II for all five energies in-

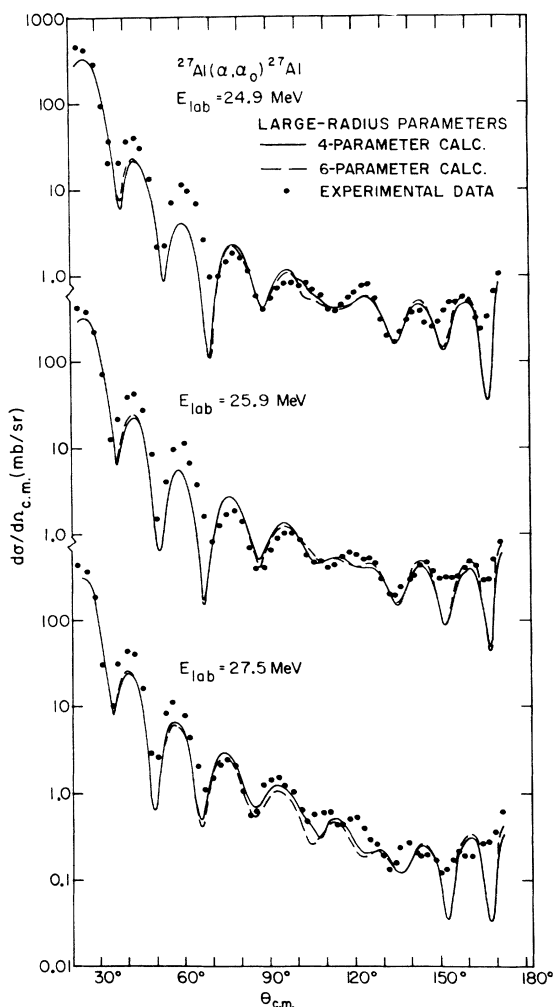


FIG. 3. Angular distributions for $^{27}\text{Al}(\alpha, \alpha_0)^{27}\text{Al}$ with optical parameters from Table I. The calculated distribution shown was with the set having $U = 194.5$ MeV.

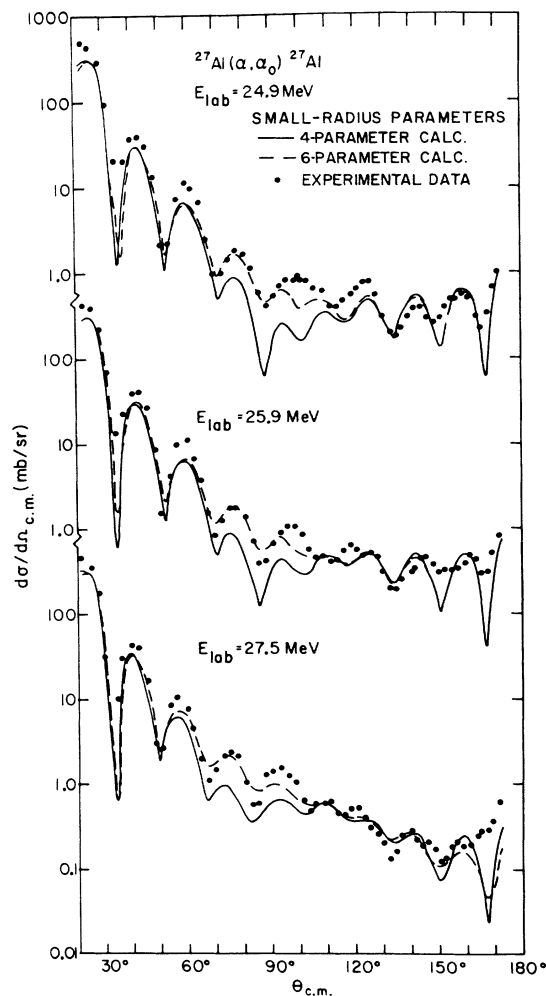


FIG. 4. Angular distributions for $^{27}\text{Al}(\alpha, \alpha_0)^{27}\text{Al}$ with the calculated distribution for $U = 217.7$ typical of the small-radius parameter sets in Table I.

TABLE II. Optical-model potential parameters with $r_I \neq r_r$ and $a_I \neq a_r$.

U (MeV)	r_r (fm)	a_r (fm)	W_1 (MeV)	W_2 (MeV)	r_I (fm)	a_I (fm)	$\bar{\chi}^2(1)$	$\bar{\chi}^2(2)$
32.0	1.68	0.56	-4.21	0.73	1.41	0.82	3480	4020
68.1	1.58	0.55	-0.48	0.64	1.39	0.72	3800	5030
108.1	1.53	0.53	2.40	0.66	1.35	0.63	4140	6000
149.0	1.52	0.50	4.55	0.79	1.31	0.24	4360	6100
194.0	1.53	0.49	0.54	0.55	1.81	0.24	4450	5460
65.1	1.31	0.86	-19.53	1.77	1.13	0.86	3750	4890
112.9	1.25	0.77	-30.23	2.90	0.90	0.80	3190	4800
164.0	1.23	0.72	-27.63	3.23	0.85	0.69	3000	4600
215.0	1.24	0.67	-24.62	3.10	0.94	0.22	2790	4500

icates that the shallowest potential describes the data best. This conclusion, however, rests on the assumption that nondirect effects are negligible at 23.3 and 22.3 MeV. In Fig. 5, the calculated cross section for the 32- and 194-MeV large-radius parameter sets of Table II are shown. For the small-radius parameters, no particular parameter set is singled out by the inclusion of the lower-energy data.

V. CONCLUSION

The scattering of α particles by ^{27}Al appears to be direct and describable with moderate success by the optical model for α -particle energies greater than 25 MeV over the angular range 20–120° (c.m.). For angles greater than 120° qualitative differences between the calculation and the data exist which could be due to a target-spin effect. In addition, the optical-model analysis of the data has shown an ambiguity in the radius parameter as well as the normally reported discrete real potential ambiguities. For the potential parameter sets with the larger radius the energy dependence of the data over the range from 22.3 to 27.5 MeV indicates a preference for the shallowest potential set, while for the smaller-radius parameters the energy dependence of the data does not indicate any potential set preference.

Below 25 MeV, the nature of the scattering mechanism is uncertain, since an anomaly has been observed at 24 MeV that cannot be repro-

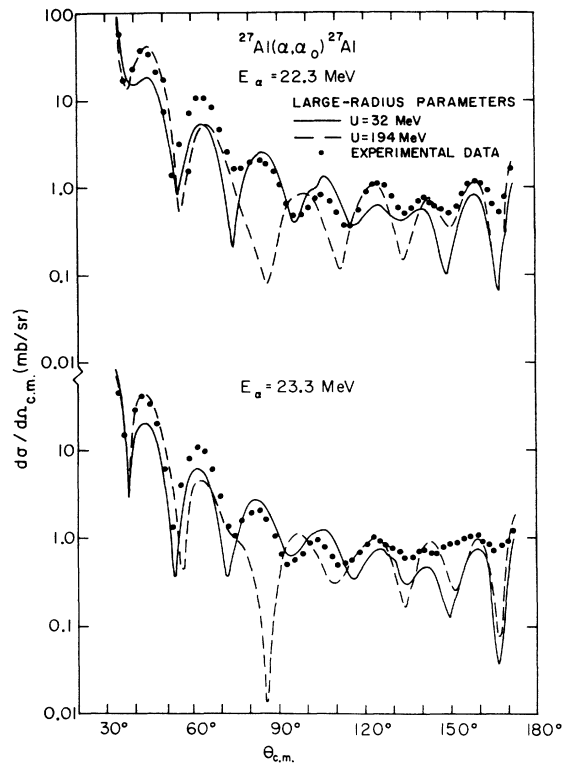


FIG. 5. Angular distributions for $^{27}\text{Al}(\alpha, \alpha_0)^{27}\text{Al}$ with a comparison of calculated angular distributions for the potential sets in Table II with $U = 32.0$ and $U = 194.0$

duced by optical-model calculations. The anomaly has a width characteristic of intermediate structure; however, the origin of this structure is at present unknown. Studies of α scattering from ^{31}P and ^{25}Mg are being undertaken to see if this type of structure is present for these nuclei also.

ACKNOWLEDGMENTS

The authors wish to thank G. Gunn, S. Marsh, D. Oliver, and T. Schmick for their willing and able assistance in taking the data. We also wish to acknowledge many stimulating discussions with Professor R. H. Davis, Professor S. Edwards, and Professor J. D. Fox on the nature of the anomalous structure seen in this work.

*Work supported in part by the Air Force Office of Scientific Research, Office of Aerospace Research, United States Air Force, under Grant No. AF-AFOSR-71-2096 and by the National Science Foundation under Grants Nos. GU-2612, GP-25974, and GJ-367.

¹M. Ivascu, G. Semencescu, D. Bucurescu, and

M. Titirici, *Rev. Roum. Phys.* **14**, 129 (1969); M. A. Ijaz, P. B. Weiss, R. H. Davis, and R. Ijaz, *J. Nat. Sci. Math.* **4**, 1 (1964).

²O. H. Gailar, E. Bleuler, and D. J. Tendam, *Phys. Rev.* **112**, 1989 (1958).

³I. Kumabe, H. Ogata, M. Inoue, Y. Okuma, and

J. Muto, J. Phys. Soc. Japan **19**, 147 (1964); J. Kokame, K. Fukunaga, and H. Nakamura, Phys. Letters **14**, 234 (1965).

⁴B. B. Srivastava and O. E. Johnson, Phys. Rev. **166**, 1083 (1968).

⁵G. R. Satchler, Nucl. Phys. **70**, 177 (1965).

⁶J. W. Frickey, K. A. Eberhard, and R. H. Davis, Phys. Rev. C **4**, 434 (1971); K. A. Eberhard and D. Robson, *ibid.* **3**, 149 (1971).

⁷G. W. Farwell and H. E. Wegner, Phys. Rev. **93**, 356 (1954).

⁸E. J. Feldl, P. B. Weiss, and R. H. Davis, Nucl. Instr. Methods **28**, 309 (1964).

⁹S. Edwards, Nucl. Phys. **A107**, 523 (1968).

¹⁰C. M. Perey and F. G. Perey, Phys. Rev. **134**, B353 (1963).

¹¹O. F. Nemets and A. T. Rudchik, Yadern Fiz. **4**, 970 (1966) [transl.: Soviet J. Nucl. Phys. **4**, 694 (1967)].

¹²C. B. Fulmer and J. C. Hafele, ORNL Report No. ORNL-4649 (unpublished); Bull. Am. Phys. Soc. **16**, 646 (1971).

¹³K. A. Eberhard, P. von Brentano, M. Böhning, and R. O. Stephen, Nucl. Phys. **A125**, 673 (1969).

¹⁴A. Bobrowska, A. Budzanowski, K. Grotowski, L. Jarczyk, B. Kamys, S. Micek, M. Polok, A. Strzalkowski, and Z. Wrobel, Institute of Nuclear Physics, Krakow, Report No. 777/PL, 1971 (unpublished).

Systematic Distorted-Wave Born-Approximation Predictions for Two-Nucleon Transfers: Applications to (d, α) Experiments*

R. M. DeVecchio and W. W. Daehnick

Nuclear Physics Laboratory, University of Pittsburgh, Pittsburgh, Pennsylvania 15213

(Received 12 June 1972)

In the case of angular-momentum-mismatch conventional distorted-wave Born-approximation (DWBA) calculations tend to give results which are strongly dependent on the optical-model parameters chosen and, to a lesser degree, on finite-range and nonlocality effects. We discuss reasons for this sensitivity and present systematic calculations for (d, α) reactions on nondeformed targets ranging from ^{48}Ti to ^{208}Pb . Satisfactory DWBA results could be obtained for the entire range of targets, provided that *all* potentials for the generation of scattered and bound wave functions were restrained to have nearly identical physically meaningful real well geometries and real depths of $V \approx nV_0$, where V_0 is the proton scattering potential and n is the number of nucleons in the projectile. The use of well geometries with $r_0 = 1.2$ fm, $a = 0.75$ fm, and retention of the basic DWBA requirement that the optical potentials should also correctly fit elastic scattering removes the familiar ambiguities for deuteron and α potentials. It is shown that with these parameter restrictions finite range effects are expected to be small so that a first-order correction procedure is adequate. Explicit calculations are compared with over 30 (d, α) angular distributions of known angular momentum transfer for experimental bombarding energies ranging from 12 to 17 MeV. Consistent agreement with experiment was obtained.

I. INTRODUCTION

Previous experience by many investigators has shown that distorted-wave Born-approximation (DWBA) calculations tend to predict transfer reactions well if, in a semiclassical view, conservation of angular momentum permits a (short range) interaction to take place at the nuclear surface. This situation is often referred to as "angular momentum matching" and leads to strongly structured angular distributions with a distinct dependence on L , the angular momentum of the transferred particle or cluster of particles. In such cases, the neglect of finite-range and nonlocality effects, or the use of a rather wide range of "reasonable" optical-model parameters for the generation of the scattered waves may have only a minor effect on

the DWBA predictions. However, for any particular experiment, good angular momentum matching is rarely possible over a broad range of L transfers or excitation energies.

The problem of angular momentum mismatch can be especially severe for (d, α) reactions. The attempt to obtain "good" DWBA calculations for such data can become a time consuming one of trial and error, sometimes involving special assumptions for the nucleus studied. DWBA then tends to lose much of its predictive value and safe L -transfer assignments require additional knowledge of the final states studied, e.g., prior knowledge of their parity. It is well known that for angular momentum mismatch the reaction cross sections are significantly affected by contributions from the nuclear interior.^{1,2} Thus details of the